

NANO IDEA

Open Access



Ultra-Sensitive Strain Sensor Based on Flexible Poly(vinylidene fluoride) Piezoelectric Film

Kai Lu^{1,2}, Wen Huang^{1*}, Junxiong Guo¹, Tianxun Gong¹, Xiongbang Wei¹, Bing-Wei Lu³, Si-Yi Liu³ and Bin Yu⁴

Abstract

A flexible 4 × 4 sensor array with 16 micro-scale capacitive units has been demonstrated based on flexible piezoelectric poly(vinylidene fluoride) (PVDF) film. The piezoelectricity and surface morphology of the PVDF were examined by optical imaging and piezoresponse force microscopy (PFM). The PFM shows phase contrast, indicating clear interface between the PVDF and electrode. The electro-mechanical properties show that the sensor exhibits excellent output response and an ultra-high signal-to-noise ratio. The output voltage and the applied pressure possess linear relationship with a slope of 12 mV/kPa. The hold-and-release output characteristics recover in less than 2.5 μs, demonstrating outstanding electro-mechanical response. Additionally, signal interference between the adjacent arrays has been investigated via theoretical simulation. The results show the interference reduces with decreasing pressure at a rate of 0.028 mV/kPa, highly scalable with electrode size and becoming insignificant for pressure level under 178 kPa.

Keywords: Piezoelectricity, PVDF film, Tactile pressure, Flexible sensor

Background

Poly(vinylidene fluoride) (PVDF) is a chemically stable piezoelectric polymer material that has many applications in different fields for its pyroelectric, piezoelectric, and ferroelectric properties [1, 2]. Especially, owing to the outstanding mechanical properties (the Young's modulus 2500 MPa and strength at break point ~ 50 MPa), the pressure sensor based on PVDF shows a good mechanical property such as flexibility and anti-fatigue [3, 4]. Compared with the commonly used pressure sensors based on ferroelectric PZT family materials, the PVDF-based pressure sensor is nontoxic and biocompatible [5, 6]. Most importantly, the PVDF-based sensor was more soft and tough than PZT-based sensor due to the high flexibility coefficient of PVDF film, which could be made the required shapes for complex strain sensing [7, 8]. Accordingly, the PVDF-based pressure sensor is thought to be one of the potential flexible bio-sensor for pressure characterization in the rapid development of

bio-medical field [9, 10]. Sharma et al. designed a pressure sensor for smart catheter with PVDF film; it could be integrated onto a catheter for real-time pressure measurement [11]. Bark et al. developed a pulse wave sensor system to non-intrusively measure heart pulse wave signals from driver's palms based on PVDF; results show that the sensor system can provide clear pulse wave signals for heart rate variability analysis, which can be used to detect driver's vigilant state to avoid traffic accidents [12]. Lee et al. fabricated a sensor with PVDF and ZnO nanostructures and it could detect the changes in pressure and temperatures for artificial skin [13]. The sensor, however, only detects pressure at a single point with large dimension.

Real-world applications, such as patched biosensor for detecting the human body pressure, demand multipoint sensing, structural flexibility, and ultra-high sensitivity [14–16]. In this reported work, a 4 × 4 flexible sensor array based on piezoelectric PVDF film is demonstrated, showing ultra-high sensitivity of 12 mV/kPa and fast output response of 2.5 μs. The magnitude and spatial distribution of the pressure applied on a human finger are characterized.

* Correspondence: uestchw@uestc.edu.cn

¹State Key Laboratory of Electronic Thin Films and Integrated Devices, University of Electronic Science and Technology of China, Chengdu 610054, China

Full list of author information is available at the end of the article

Design and Experimental

Design and Fabrication of the Sensor Array

The proposed sensor array has a sandwich structure based on a PVDF thin film with the thickness of about 50 μm (Jinzhou Kexin Inc., China). The aluminum electrode arrays with the thickness of 20 μm were covered on both sides of the PVDF film. Figure 1a shows a schematic design of the sensor. The sensor has 16 micro-capacitor units; every 4 units share one connecting wire to minimize the amount of the electrode wires.

To fabricate the sensor array, a slide glass covered with polydimethylsiloxane (PDMS) was prepared as a stiff substrate. The PVDF thin film covered by Al on both sides was loaded on the substrate. Then, the photoresist was spin-coated on the surface of the film with a speed of 3000 rpm for 40 s. After photolithography and wet etching of Al by a mask aligner system (ABM, Inc., USA), the 16 capacitor units with 4×4 square structure were prepared. After that, the flexible sensor on the PDMS substrate was picked up from the slide glass. The electrodes of each capacitor were connected with the conductive wires through silver glue. In order to obtain good bio-compatibility, the sensor was packaged by being covered with PDMS on the top and heated for 12 h at 60 $^{\circ}\text{C}$. Figure 1b displays a photograph of the bent pressure sensor, illuminating that the sensor is flexible.

Piezoelectric Property of the Sensor Array Based on the PVDF Film

Piezoresponse force microscopy (PFM) study (Seiko, Inc., Japan) was carried out to characterize the surface morphology and piezoelectric properties of the PVDF film of the proposed sensor under an AC bias voltage of 2 V with a scanning area size of $2 \times 2 \mu\text{m}^2$.

Calibration for the Sensor Array

To calibrate the sensor, various pressures were applied on the proposed sensor in an electro-mechanical experimental platform connecting to a data acquisition (DAQ-USB6008) equipment from National Instruments. The

data acquisition with four differential analog signals was set with differential model. The output voltage signal from the proposed sensor was obtained by changing the connection between sensor array and the DAQ.

Results and Discussion

Figure 2a shows the surface morphology of the sensor after etching of Al, checked by an optical microscope. The fairly bright and dark contrast suggests a clear interface between PVDF and the etched Al electrodes. Figure 2b, c shows the surface morphology and phase signal of the PVDF film of the pressure sensor. It is indicated that the surface of PVDF is smooth with a tissue structure. The phase image of PFM measure in Fig. 2c shows a strong response of the piezoelectric domain which is consistent with the surface structure seen in Fig. 2b. These results suggest that the as-prepared sensor based on the PVDF film exhibits a good piezoelectricity.

A typical result of the output signal is shown in Fig. 3a when a constant pressure of 98.1 kPa was applied on one of the squared electrode of the sensor [17]. The x -axis and y -axis show the time and the output voltage of the squared electrode of the sensor, respectively. The output voltage was converted from charge (Q) generated by the PVDF film of the sensor. Based on the piezoelectricity equation (where d_{33} is a piezoelectric constant when the direction of polarization is the same with the direction of electric field and F_z means pressure is applied on the z -direction with the same direction of d_{33}), a relation between output voltage and pressure could be established. The raw data were obtained by applying a band block of 49–51 Hz. The arrow line of this figure indicates the signals of about 123.1 mV which was generated by the pressure applied on the sensor. The output voltage of the sensor by the pressure is shown clearly in the signal with low noise and high signal-to-noise ratio. In order to confirm the synchronal property of the sensor array, an equal pressure of 113.2 kPa was applied on four units of the sensor, simultaneously. The output voltage signals induced by the pressure were showed in Fig. 3b. The nearly same output

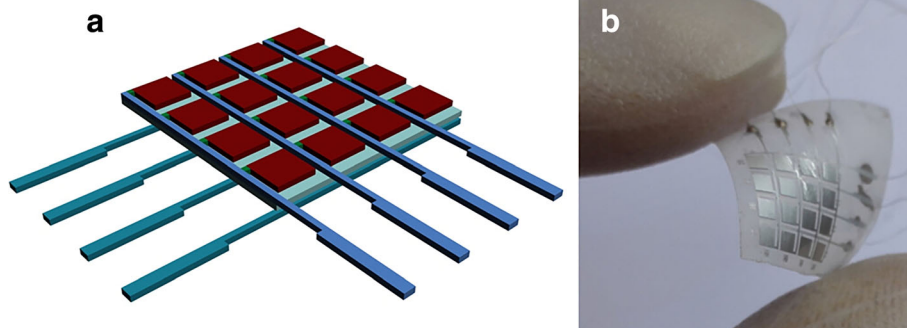
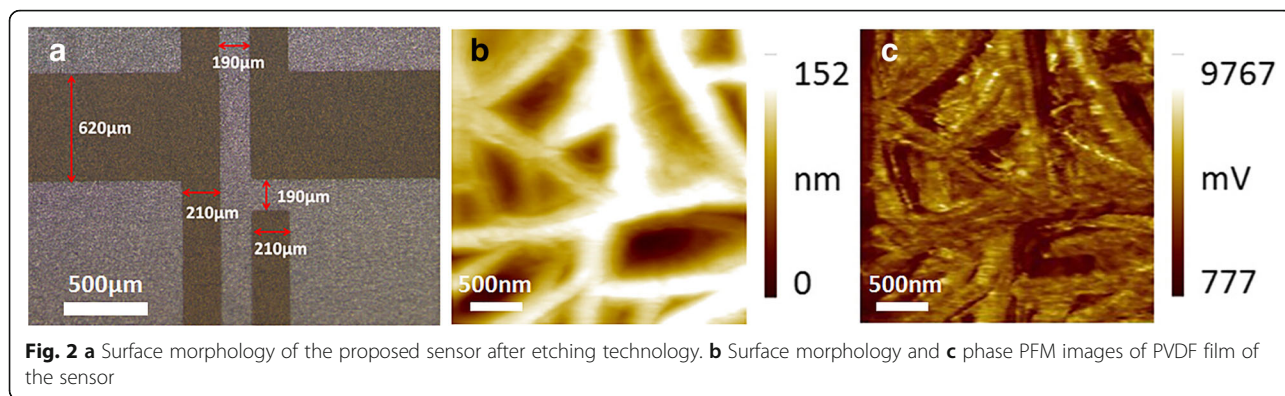


Fig. 1 a Schematic diagram of the sensor array. b Physical picture of the ultimate device

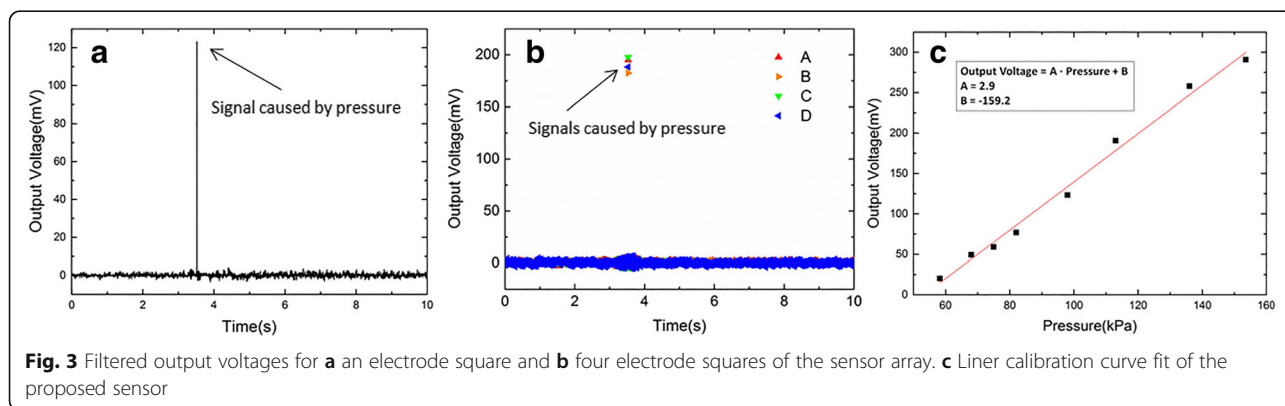


value of about 190 mV was obtained from the four units of the sensor at the same time, which suggests that the sensor array exhibited a high stability and synchronal property by applying multipoint pressure. For calibrating the sensor array, different pressures in the range of 60–150 kPa were applied on the sensor array; the output voltage vs. the applied pressure were obtained and plotted as the calibration curve shown in Fig. 3c, which exhibits a linear relationship. The slope of the linear curve is about 2.9 mV/kPa, and there is an offset of -159.2 mV in the calibration curve.

The hold-and-release output response of one squared electrode of the sensor was obtained by applying an impulse pressure with various frequencies. The plotted curve in Fig. 4a shows the typical response of the sensor by applying the impulse pressure of about 75.1 kPa with a frequency of 90 Hz. The positive output voltage corresponds to the compression of the electrode square of the sensor array, and the negative output voltage corresponds to the relaxation. As seen in the inset of Fig. 4a, the similar hold-and-release output response has also been observed in the bare piezoelectric PVDF film [18]. The response time of output voltage of the sensor is less than 2 ms, which suggests the sensor exhibits a good electro-mechanical response property. The impulse pressures within the range of 60–150 kPa were applied on the sensor array. The hold-and-release

output response curves were shown in Fig. 4b. The sensor shows a stable characteristic of electro-mechanical response with the response time of about 2 ms under different pressures, and the output voltages of the sensor under different pressures are consistent with the linear calibration curve obtained above.

Next, application of pressure on selective point is studied. Signal interference is shown between the adjacent arrays, when pressure was applied on the electrode of one of the arrays. The simulation of signal interference was conducted via COMSOL Multiphysics on arrays. Each electrode area is 1.4 mm². The geometry of the structure is shown in Fig. 5a. The additional strain, when pressure was applied on electrode A, is seen in Fig. 5b, indicating the strain increases with the distance away from electrode A. The interference in potential difference with a pressure level of 20~80 kPa was studied, shown in Fig. 5c. The potential difference and pressure exhibit a linear relationship with a slope of 0.028 mV/kPa and an intercept of 5×10^{-4} mV, implying very-low-level interference. A pressure under 178 kPa would generate signal interference less than 5 mV which is negligible [16, 17]. In addition, the dependence of interference on array electrode size has been investigated. Figure 5d shows the result with electrode sizes of 1.2, 1.0, and 0.8 mm². It shows that a linear relationship between interference potential difference and pressure (in the range



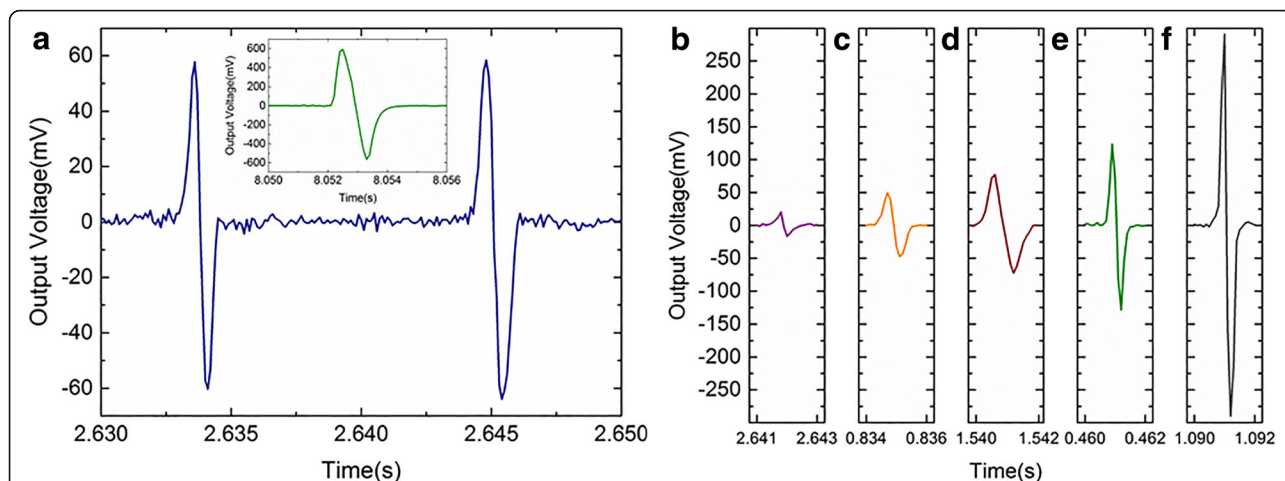


Fig. 4 The hold-and-release output response from the pressures of **a** 75.1 kPa, **b** 58.2 kPa, **c** 67.8 kPa, **d** 81.9 kPa, **e** 98.1 kPa, and **f** 153.6 kPa; the inset shows the hold-and-release output response obtained from bare PVDF film

of 20~60 kPa) can be still observed in the smallest electrode. The fitting slopes for interface voltage are 0.01748, 0.01181, and 0.00574 mV/kPa, respectively, for the three structures with the noted observation of reduced interference potential in smaller electrode size.

For a simple practical application, the sensor was applied to measure the pressure state and distribution of the finger of human hand. As we all have known, the complex finger movement consists of some basic skills, such as shiatsu, kneading, rub, friction, and so on [19]. In our experiments, three most commonly used movements including shiatsu, kneading, and rub were selected to test the pressure state

and distribution of the finger. Figure 6 shows a snap of the pressure distribution of the thumb finger characterized by the sensor during the three movements of the finger, respectively. In Fig. 6a, it could be clearly seen that the pressure of 76 kPa was focused in the center of the thumb finger during the shiatsu movement, which are quite different with the kneading and the rub seen in Fig. 6b, c, respectively. Figure 6b shows the pressure from the front of the thumb finger is higher than the other parts of the finger during the kneading movement, while the pressure of the thumb finger is fairly uniform (about 68 kPa) during the rub movement as shown in Fig. 6c. The observed pressure

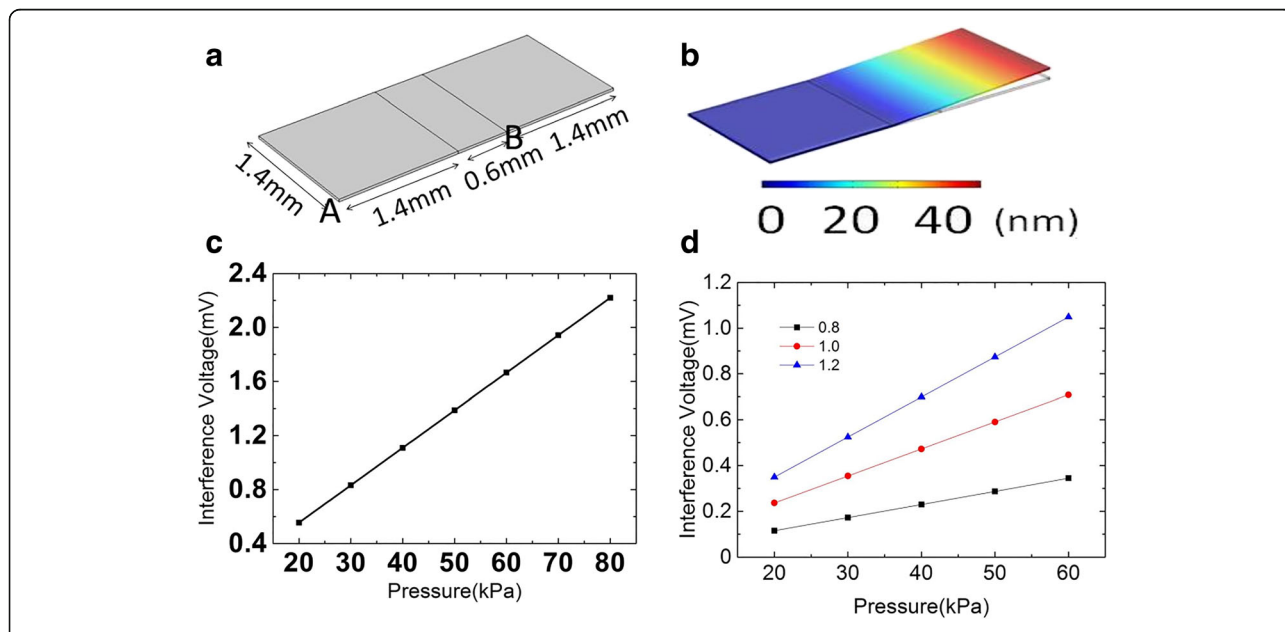
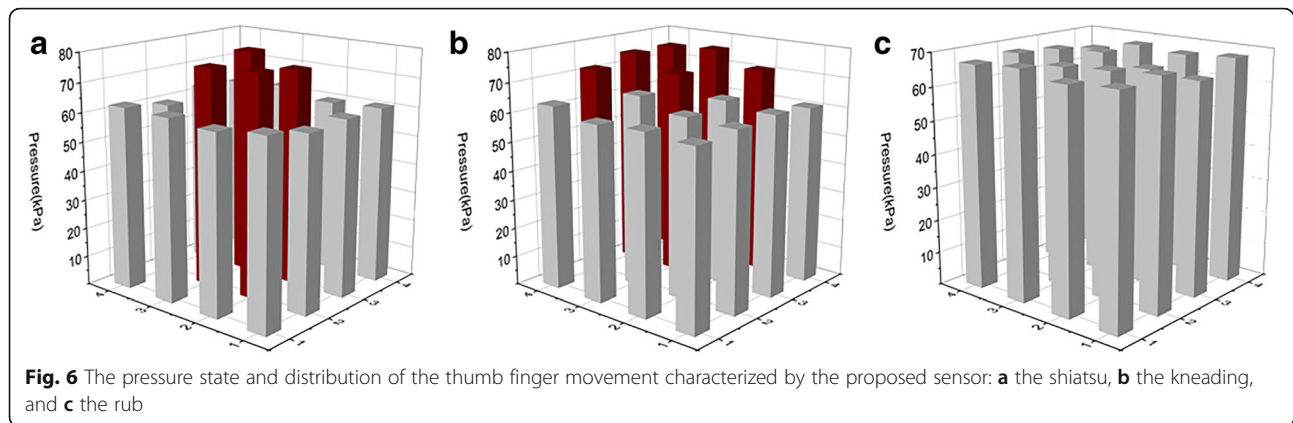


Fig. 5 **a** Physical dimensions used for theoretical simulation. **b** Displacement and **c** liner curve-fitting between interference voltage and applied pressure with an array size of 1.4 mm. **d** Obtained results using array sizes of 0.8, 1.0, and 1.2 mm, respectively



distribution in the finger is somewhat similar with the previous reports in clinical observation [17, 20]. According to our measurements, the strain sensor based on flexible ferroelectric PVDF film prove to be sensitive for characterize the complex finger movement. It is expected to explore the skill of the human finger more precisely by using the proposed sensor, and it would also be helpful to develop the robot to replace human fingers in the future.

In conclusion, a 4×4 sensor array with 16 capacitor units based on the piezoelectric PVDF thin film has been fabricated and packaged with PDMS. The sensor array exhibits flexible and high sensitive properties. The hold-and-release output response of the sensor was obtained by applying impulse pressures with various frequencies, which indicated the sensor array could generate 20–300 mV voltage signals within 2 ms when applying a pressure in the range of 60–150 kPa. The obviously different pressure distributions in the finger during the finger movement of human hand have been observed by using the proposed sensor, which is expected to explore the skill of the human fingers more precisely.

Abbreviations

PFM: Piezoresponse force microscopy; PVDF: Poly(vinylidene fluoride)

Funding

The project was supported by research grants from the open fund of the State Key Laboratory of Luminescent Materials and Devices (No. 2018-sk1md-06), the Fundamental Research Funds for the Central Universities (Nos. ZYGX2016J055 and ZYGX2016KYQD131), and the Technology Innovative Research Fund of Sichuan Province of China (Grant No. 2015TD0005). This work was also supported by the National Natural Science Foundation of China (Grant No. 61474016).

Availability of data and materials

The datasets generated during and/or analyzed during the current study are available from the corresponding authors on reasonable request.

Authors' contributions

KL and WH designed the experiments and wrote the manuscript. KL and JXG designed and performed the sample fabrication. TXG performed and analyzed the surface morphology of the sensor. XBW and BWL performed and analyzed the piezoelectric results. SYL and BY performed and analyzed the mechanical experiment. All authors contributed to the scientific discussion and edited the manuscript. All authors read and approved the final manuscript.

Competing interests

The authors declare that they have no competing interests.

Publisher's Note

Springer Nature remains neutral with regard to jurisdictional claims in published maps and institutional affiliations.

Author details

¹State Key Laboratory of Electronic Thin Films and Integrated Devices, University of Electronic Science and Technology of China, Chengdu 610054, China. ²State Key Laboratory of Luminescent Materials and Devices, South China University of Technology, Guangzhou 510006, China. ³AML, Department of Engineering Mechanics, Tsinghua University, Beijing 100084, China. ⁴College of Nanoscale Science and Engineering (CNSE), State University of New York, Albany, NY 12203, USA.

Received: 1 February 2018 Accepted: 2 March 2018

Published online: 14 March 2018

References

- Harris GR, Preston RC, DeReggi AS (2000) The impact of piezoelectric PVDF on medical ultrasound exposure measurements, standards, and regulations. *IEEE Trans Ultrason Ferroelectr Freq Control* 47(6):1321–1335
- Nakamachi E, Uetsuji Y, Kuramae H, Tsuchiya K, Hwang H (2013) Process crystallographic simulation for biocompatible piezoelectric material design and generation. *Arch Comput Meth Eng* 20(2):155–183
- Fukada E (2000) History and recent progress in piezoelectric polymers. *IEEE Trans Ultrason Ferroelectr Freq Control* 47(6):1277–1290
- Meng Y, Yi W (2011) Application of a PVDF-based stress gauge in determining dynamic stress–strain curves of concrete under impact testing. *Smart Mater Struct* 20(6):065004
- Cauda V, Canavese G, Stassi S (2015) Nanostructured piezoelectric polymers. *J Appl Polym Sci* 132(13)
- Shu FF (2007) Application of PVDF piezoelectric-film sensor to plantar pressure measurement. In 6th China International Silk Conference/2nd International Textile Forum, pp 322–326
- Liu X, Liu S, Han MG, Zhao L, Deng H, Li J, Zhu Y, Krusin-Elbaum L, O'Brien S (2013) Magnetolectricity in CoFe_2O_4 nanocrystal-P (VDF-HFP) thin films. *Nanoscale Res Lett* 8(1):374
- Jo SH, Lee SG, Lee YH (2012) Ferroelectric properties of PZT/BFO multilayer thin films prepared using the sol-gel method. *Nanoscale Res Lett* 7(1):54
- Tonazzini I, Bystrenova E, Chelli B, Greco P, De Leeuw D, Biscarini F (2015) Human neuronal SHSY5Y cells on PVDF: PTrFE copolymer thin films. *Adv Eng Mater* 17(7):1051–1056
- Li F, Liu WT, Stefanini C, Fu X, Dario P (2010) A novel bioinspired PVDF micro/nano hair receptor for a robot sensing system. *Sensors* 10(1):994–1011
- Sharma T, Aroom K, Naik S, Gill B, Zhang JXJ (2013) Flexible thin-film PVDF-TrFE based pressure sensor for smart catheter applications. *Ann Biomed Eng* 41(4):744–751

12. Baek HJ, Chung GS, Kim KK, Park KS, Smart Health A (2012) Monitoring chair for noninvasive measurement of biological signals. *IEEE Trans Inf Technol Biomed* 16(1):150–158
13. Lee JS, Shin KY, Cheong OJ, Kim JH, Jang H (2015) Highly sensitive and multifunctional tactile sensor using free-standing ZnO/PVDF thin film with graphene electrodes for pressure and temperature monitoring. *Sci Report* 5: 7887
14. Moyer CA, Rounds J, Hannum JW (2004) A meta-analysis of massage therapy research. *Psychol Bull* 130(1):3–18
15. Ferrelltorry AT, Glick OJ (1993) The use of therapeutic massage as a nursing intervention to modify anxiety and the perception of cancer pain. *Cancer Nurs* 16(2):93–101
16. Ryu J, Son J, Ahn S, Shin I, Kim Y (2015) Biomechanical analysis of the circular friction hand massage. *Technology & Health Care Official Journal of the European Society for Engineering & Medicine* 23 Suppl 2(s2):S529
17. Shirafuji S, Hosoda K. Detection and prevention of slip using sensors with different properties embedded in elastic artificial skin on the basis of previous experience. In *International Conference on Advanced Robotics*. 2014
18. Sharma T, Je SS, Gill B, Zhang JXJ (2012) Patterning piezoelectric thin film PVDF-TrFE based pressure sensor for catheter application. *Sensors and Actuators a-Physical* 177:87–92
19. Furlan AD, Brosseau L, Imamura M, Irvin E (2002) Massage for low-back pain: a systematic review within the framework of the Cochrane Collaboration Back Review Group. *Spine* 27(17):1896–1910
20. Liao X, Ava L, Nicola R (2011) The evidence for shiatsu: a systematic review of shiatsu and acupressure. *Bmc Complementary & Alternative Medicine* 11(1):88

Submit your manuscript to a SpringerOpen[®] journal and benefit from:

- ▶ Convenient online submission
- ▶ Rigorous peer review
- ▶ Open access: articles freely available online
- ▶ High visibility within the field
- ▶ Retaining the copyright to your article

Submit your next manuscript at ▶ springeropen.com
